Chapter 4

Compact stars with charged distributions on pseudo-spheroidal spacetime

In this chapter, we have studied two models of charged anisotropic fluid distributions on the background of a pseudo-spheroidal spacetime by assuming two different expressions for pressure distribution and electric field intensity. The physical acceptability of the models are investigated and found that they are compatible with a number of pulsars of known mass and size.

4.1 Introduction

The equilibrium of a spherical distribution of matter in the form of perfect fluid is maintained by the repulsive pressure force against the gravitational attraction. For matter distribution in the form of dust, there is no such force to counter the gravitational attraction. In such situations, the collapse of the distribution to a singularity can be averted if the matter is accompanied by some electric charge. The

Coulombian force of repulsion due to the presence of charge contributes additional force to the fluid pressure when the matter is in the form of perfect fluid.

A systematic study of electromagnetic fields in the context of general relativity was due to Rainich [1925]. The equilibrium of charged dust spheres within the frame work of general relativity was examined critically by Papapetrou [1947] and Majumdar [1947]. Bonner [1960, 1965] has shown that a spherical distribution of matter can keep its equilibrium if it is accompanied by electric charge. Stettner [1973] has shown that a uniform density fluid distribution accompanied by some surface charge is more stable than the one without charge. Krori and Barua [1975] obtained a singularity free solution for static charged fluid spheres. This solution has been analysed in detail by Juvenicus [1976]. The solution obtained by Pant and Sah [1979] for static spherically symmetric relativistic charged fluid sphere has Tolman Solution VI as a particular case in the absence of charge.

Cooperstock and de la. Cruz [1978] have studied relativistic spherical distributions of charged perfect fluids in equilibrium and obtained explicit solutions of Einstein - Maxwell equations in the interior of a sphere containing uniformly charged dust in equilibrium. Bonnor and Wickramsuriya [1975] have obtained a static interior dust metric with matter density increasing outward. Whitman and Burch [1981] have given a method for solving coupled Einstein - Maxwell equations for spherically symmetric static systems containing charge, obtained a number of analytic solutions and examined their stability. Conformally flat interior solutions were obtained by Chang [1983] for charged fluid as well as charged dust distributions.

Tikekar [1984] has studied some general aspects of spherically symmetric static distributions of charged fluids for specific choice of density and pressure. This solution admits Pant and Sah [1979] solution as a particular case. Patel and Mehta [1995] have obtained solutions of Einstein - Maxwell equations. J. K. Rao and Trivedi

[2000] have developed a formalism for generating new solutions of coupled Einstein - Maxwell equations.

The study of charged superdense star models compatible with observational data has generated deep interest among researchers in the recent past and a number of articles have been appeared in this direction Maurya and Gupta [2011a,b,c], Pant and Maurya [2012], Maurya et al. [2017b]. Theoretical investigations of Ruderman [1972] and Canuto [1974] suggest that matter may not be isotropic in high density regime and hence it is pertinent to study charged models incorporating anisotropy in pressure. Relativistic models of charged fluids distributions on spacetimes with spheroidal geometry have been studied by Patel and Koppar [1987], Tikekar and Singh [1998], Sharma et al. [2001], Gupta and Kumar [2005] and Komathiraj and Maharaj [2007a].

Charged strange and quark star models have been studied by Sharma et al. [2006], and Sharma and Mukherjee [2001, 2002]. The study of charged fluid distributions have been carried out recently by Maurya and Gupta [2011a,b,c], Pant and Maurya [2012] and Maurya et al. [2017b].

In the present chapter, we have obtained new class of solutions for charged fluid distribution on the background of pseudo spheroidal spacetime. Particular choices for radial pressure p_r and electric field intensity E are taken so that the physical requirements and regularity conditions are not violated. The bounds for the geometric parameter K and the parameter α associated with charge, are determined using various physical requirements that are expected to satisfy in its region of validity. It is found that these models can accommodate a number of pulsars like like 4U 1820-30, PSR J1903+327, 4U 1608-52, Vela X-1, SMC X-4, Cen X-3, given by Gangopadhyay et al. [2013]. When $\alpha = 0$, the model reduces to the uncharged anisotropic distribution given by Thomas and Pandya [2015a].

4.2 Field Equations

We shall take the interior spacetime metric representing charged anisotropic matter distribution as

$$ds^2 = e^{\nu(r)}dt^2 - \left(\frac{1+K\frac{r^2}{R^2}}{1+\frac{r^2}{R^2}}\right)dr^2 - r^2\left(d\theta^2+\sin^2\theta d\phi^2\right), \tag{4.1}$$

where K and R are geometric parameters and $K > 1$. This spacetime, known as pseudo-spheroidal spacetime, has been studied by number of researchers Tikekar and Thomas [1998, 1999, 2005], Thomas et al. [2005], Thomas and Ratanpal [2007], Paul et al. [2011], Chattopadhyay and Paul [2010], Chattopadhyay et al. [2012] and have found that it can accommodate compact superdense stars.

Since the metric potential g_{rr} is chosen apriori, the other metric potential $\nu(r)$ is to be determined by solving the Einstein-Maxwell field equations

$$R_i^j - \frac{1}{2}R\delta_i^j = 8\pi\left(T_i^j + \pi_i^j + E_i^j\right), \tag{4.2}$$

where,

$$T_i^j = (\rho+p)\,u_i u^j - p\delta_i^j, \tag{4.3}$$

$$\pi_i^j = \sqrt{3}S\left[c_i c^j - \frac{1}{2}\left(u_i u^j - \delta_i^j\right)\right], \tag{4.4}$$

and

$$E_i^j = \frac{1}{4\pi}\left(-F_{ik}F^{jk} + \frac{1}{4}F_{mn}F^{mn}\delta_i^j\right). \tag{4.5}$$

Here ρ, p, u_i, S and c^i, respectively, denote the proper density, fluid pressure, unit-four velocity, magnitude of anisotropic tensor and a radial vector given by $\left(0, -e^{-\lambda/2}, 0, 0\right)$. F_{ij} denotes the anti-symmetric electromagnetic field strength ten-

sor defined by

$$F_{ij} = \frac{\partial A_j}{\partial x_i} - \frac{\partial A_i}{\partial x_j}, \tag{4.6}$$

which satisfies the Maxwell equations

$$F_{ij,k} + F_{jk,i} + F_{ki,j} = 0, \tag{4.7}$$

and

$$\frac{\partial}{\partial x^k}\left(F^{ik}\sqrt{-g}\right) = 4\pi\sqrt{-g}J^i, \tag{4.8}$$

where g denotes the determinant of g_{ij}, $A_i = (\phi(r), 0, 0, 0)$ is four-potential and

$$J^i = \sigma u^i, \tag{4.9}$$

is the four-current vector and σ denotes the charge density.

The only non-vanishing components of F_{ij} is $F_{01} = -F_{10}$. Here

$$F_{01} = -\frac{e^{\frac{\nu+\lambda}{2}}}{r^2}\int_0^r 4\pi r^2 \sigma e^{\lambda/2} dr, \tag{4.10}$$

and the total charge inside a radius r is given by

$$q(r) = 4\pi\int_0^r \sigma r^2 e^{\lambda/2} dr. \tag{4.11}$$

The electric field intensity E can be obtained from $E^2 = -F_{01}F^{01}$, which subsequently reduces to

$$E = \frac{q(r)}{r^2}. \tag{4.12}$$

The field equations given by (4.2) are now equivalent to the following set of the non-linear ODE's

$$\frac{1 - e^{-\lambda}}{r^2} + \frac{e^{-\lambda}\lambda'}{r} = 8\pi\rho + E^2, \tag{4.13}$$

$$\frac{e^{-\lambda}-1}{r^2}+\frac{e^{-\lambda}\nu'}{r}=8\pi p_r-E^2, \tag{4.14}$$

$$e^{-\lambda}\left(\frac{\nu''}{2}+\frac{\nu'^2}{4}-\frac{\nu'\lambda'}{4}+\frac{\nu'-\lambda'}{2r}\right)=8\pi p_\perp+E^2, \tag{4.15}$$

where we have taken

$$p_r=p+\frac{2S}{\sqrt{3}}, \tag{4.16}$$

$$p_\perp=p-\frac{S}{\sqrt{3}}. \tag{4.17}$$

Because $e^{\lambda}=\frac{1+K\frac{r^2}{R^2}}{1+\frac{r^2}{R^2}}$, the metric potential λ is a known function of r. The set of equations (4.13) - (4.15) are to be solved for five unknowns ν, ρ, p_r, $p_\perp$ and E. So we have two free variables for which suitable assumption can be made.

4.3 Charged Anisotropic Model 1

We shall assume the following expressions for p_r and E with the central pressure $p_0>0$.

$$8\pi p_r=\frac{p_0\left(1-\frac{r^4}{R^4}\right)}{R^2\left(1+K\frac{r^2}{R^2}\right)^2}, \tag{4.18}$$

and

$$E^2=\frac{\alpha\ r^2}{R^4}. \tag{4.19}$$

The expressions for p_r and E^2 are so selected that it may comply with the physical requirement. A physically acceptable radial pressure p_r should be finite at the centre $r=0$, decreasing radially outward and finally vanish at the boundary of the distribution. The gradient of p_r is given by

$$8\pi\frac{dp_r}{dr}=-\frac{4\ p_0\ r\left(K+\frac{r^2}{R^2}\right)}{R^4\left(1+\frac{Kr^2}{R^2}\right)^3}. \tag{4.20}$$

It can be noticed from equation (4.18) that $8\pi p_r|_{r=0} = \frac{p_0}{R^2}$, which is a finite quantity at $r = 0$. It vanishes at $r = R$, which is taken as the boundary radius of the star. Further from equation (4.20) it can be noticed that p_r is a radially decreasing function of r. For a physically acceptable electric field intensity, $E(0) = 0$ and $\frac{dE}{dr} > 0$. From equation (4.19), it is evident that E is a monotonically increasing function of r.

On substituting the values of p_r and E^2 in (4.14) we obtain, after a lengthy calculation

$$\begin{aligned} e^{\nu} &= C \times \exp\left[-\frac{\left(1+\frac{r^2}{R^2}\right)\left(\frac{K^2\alpha r^2}{R^2}+(2p_0+(2-3K)K\alpha)\right)}{4K}\right] R^{(K-1)(1-\alpha)+\frac{(1+K)p_0}{K^2}} \\ &\quad \times \left(1+\frac{r^2}{R^2}\right)^{\frac{1}{2}(K-1)(1-\alpha)} \times \left(1+K\frac{r^2}{R^2}\right)^{\frac{(1+K)p_0}{2K^2}} \end{aligned} \tag{4.21}$$

where C is a constant of integration.

Hence, with the help of the equation (4.21), spacetime metric (4.1) can be written explicitly as

$$\begin{aligned} ds^2 &= \left\{C \times \exp\left[-\frac{\left(1+\frac{r^2}{R^2}\right)\left(\frac{K^2\alpha r^2}{R^2}+(2p_0+(2-3K)K\alpha)\right)}{4K}\right] R^{(K-1)(1-\alpha)+\frac{(1+K)p_0}{K^2}}\right. \\ &\quad \left. \times \left(1+\frac{r^2}{R^2}\right)^{\frac{1}{2}(K-1)(1-\alpha)} \times \left(1+K\frac{r^2}{R^2}\right)^{\frac{(1+K)p_0}{2K^2}}\right\} dt^2 - \left(\frac{1+K\frac{r^2}{R^2}}{1+\frac{r^2}{R^2}}\right) dr^2 \\ &\quad -r^2\left(d\theta^2+\sin^2\theta d\phi^2\right). \end{aligned} \tag{4.22}$$

The interior spacetime metric (4.22) is suitable to represent the charged fluid distribution if it match continuously with Riessner-Nordström metric

$$ds^2 = \left(1-\frac{2m}{r}+\frac{q^2}{r^2}\right)dt^2 - \left(1-\frac{2m}{r}+\frac{q^2}{r^2}\right)^{-1} dr^2 - r^2\left(d\theta^2+\sin^2\theta d\phi^2\right), \tag{4.23}$$

across the boundary $r = R$. The continuity of metric coefficients across $r = R$ provide the estimates of the constant of integration C and M as

$$C = \frac{2}{K+1}\left(R\sqrt{2}\right)^{(K-1)(\alpha-1)} e^{\frac{p_0}{K}+\alpha(1-K)}\left((1+K)R^2\right)^{-\frac{(1+K)p_0}{2K^2}} \tag{4.24}$$

and

$$M = \frac{R(\alpha(K+1)+K-1)}{2(K+1)}. \tag{4.25}$$

Here $M = m(r = R)$ denotes the mass of the star inside the radius R.

4.4 Physical Requirements and Bounds for Parameters

Now, equation (4.13) gives the density of the distribution as

$$8\pi\rho = \frac{(K-1)\left(3+K\frac{r^2}{R^2}\right)}{R^2\left(1+K\frac{r^2}{R^2}\right)^2} - \frac{\alpha\, r^2}{R^4}. \tag{4.26}$$

The condition $\rho(r = 0) > 0$ is clearly satisfied and $\rho(r = R) > 0$ gives the following inequality connecting α and K.

$$0 \leq \alpha < 1 - \frac{4}{(K+1)^2}. \tag{4.27}$$

Since $K > 1$, the inequality (4.27) implies

$$0 \leq \alpha < 1. \tag{4.28}$$

Differentiating (4.26) with respect to r, we get

$$8\pi\frac{d\rho}{dr} = -\frac{2\ r}{R^4}\left(\frac{K(K-1)\left(5+\frac{Kr^2}{R^2}\right)+\alpha}{R^4\left(1+\frac{Kr^2}{R^2}\right)^3}\right). \tag{4.29}$$

It is observed that $\frac{d\rho}{dr}(r=0)=0$ and $\frac{d\rho}{dr}(r=R)<0$. In fact ρ is a decreasing function of r throughout the distributions.

The expression for $p_\perp$ is

$$\begin{aligned} 8\pi p_\perp \ = \ & \frac{1}{2R^4}\left(\frac{p_0^2r^2\left(1-\frac{r^2}{R^2}\right)^2\left(1+\frac{r^2}{R^2}\right)}{2\left(1+\frac{Kr^2}{R^2}\right)^3}+\frac{(-1+K)^2r^2\left(3+\frac{Kr^2}{R^2}\right)}{2\left(1+\frac{r^2}{R^2}\right)\left(1+\frac{Kr^2}{R^2}\right)^2}\right. \\ & +\frac{p_0\left(-K(K+1)\frac{r^6}{R^6}+(K^2-3K-4)\frac{r^4}{R^4}-\frac{2r^2}{R^2}+2\right)}{R^{10}\left(1+\frac{Kr^2}{R^2}\right)^3} \\ & -\frac{r^2}{R^6}\frac{\left(-p_0\frac{r^6}{R^6}+K(K+5)\frac{r^4}{R^4}+(p_0+8K+4)\frac{r^2}{R^2}+6\right)\alpha}{\left(1+\frac{r^2}{R^2}\right)\left(1+\frac{Kr^2}{R^2}\right)} \\ & \left.+\frac{1}{2}\frac{r^6}{R^4}\frac{\left(1+\frac{Kr^2}{R^2}\right)\alpha^2}{\left(1+\frac{r^2}{R^2}\right)}\right). \end{aligned} \tag{4.30}$$

The condition $p_\perp > 0$ at the boundary $r=R$ imposes a restriction on α and p_0 respectively given by

$$0 \le \alpha < \frac{K^2+13K+10}{(K+1)^2} - \sqrt{\frac{24K^3+193K^2+262K+97}{(K+1)^4}} \tag{4.31}$$

and

$$0 < p_0 \le \frac{1}{16}\left(\alpha^2(K+1)^3 - 2\alpha(K(K+13)+10)(K+1)+(K-1)^2(K+3)\right). \tag{4.32}$$

The anisotropy can be written in the form

$$8\pi\sqrt{3}S = 8\pi p_r - 8\pi p_\perp. \tag{4.33}$$

The expression for $\frac{dp_\perp}{dr}$ is given by

$$\begin{aligned}
8\pi\frac{dp_\perp}{dr} &= \frac{3}{2}\left(K\alpha^2 - \frac{p_0\left(K^2-1\right)\left(6K^2 - p_0(K+1)\right)}{K\left(1+\frac{Kr^2}{R^2}\right)^4}\right)\frac{r^5}{R^8} \\
&\quad - \left(\frac{2K^4(K-1) + \left\{\left(4-K-7K^2\right)2K^2 + \left(2K^3+K^2+1\right)p_0\right\}p_0}{K^2\left(1+\frac{Kr^2}{R^2}\right)^3}\right. \\
&\quad \left. + \frac{\alpha(K\alpha(K-1)-2p_0)}{K}\right)\times\frac{r^3}{R^6} \\
&\quad + \left(\frac{K^4(3K-5) - 4K^3p_0(1+3K) + p_0^2\left(K^3-1\right) + 2K\alpha\left(K^2+p_0(K+1)\right)}{2K^3\left(1+\frac{Kr^2}{R^2}\right)^2}\right. \\
&\quad - \frac{(\alpha-1)(3-K+\alpha(K-1))}{2\left(1+\frac{r^2}{R^2}\right)^2} \\
&\quad \left. + \frac{p_0^2 - K\alpha\left(2\left(K^3+5K^2+p_0(K+1)\right)K\alpha - K^3\alpha^2(K-1)\right)}{2K^3}\right)\times\frac{r}{R^4}.
\end{aligned} \tag{4.34}$$

Evidently, the value of $\frac{dp_\perp}{dr} = 0$ at the origin; and at the boundary $\frac{dp_\perp}{dr}(r=R) < 0$ gives the following bounds for α with $p_0 > 0$

$$0 \leq \alpha \leq \frac{K(K-3)+10}{(K+1)^2}. \tag{4.35}$$

Using (4.28) in above inequality (4.35), we get

$$K > 1.8 \tag{4.36}$$

a lower bound for K.

In order to examine the strong energy condition, we evaluate the expression $\rho - p_r - 2p_\perp$ at the centre and on the boundary of the star. It is found that, for a positivity

of $\rho - p_r - 2p_\perp$ at the centre,

$$0 < p_0 < K - 1, \tag{4.37}$$

and $(\rho - p_r - 2p_\perp)\,(r = R) > 0$ gives the bound on K and α, namely

$$1 < K \leq 5, \tag{4.38}$$

$$0 \leq \alpha \leq \frac{K^2 + 11K + 8}{(K+1)^2} + \sqrt{\frac{24K^3 + 153K^2 + 174K + 49}{(K+1)^4}}. \tag{4.39}$$

The expressions for adiabatic sound speed $\frac{dp_r}{d\rho}$ and $\frac{dp_\perp}{d\rho}$ in the radial and transverse directions, respectively, are given by

$$\frac{dp_r}{d\rho} = \frac{2p_0\left(K + \frac{r^2}{R^2}\right)}{(K-1)K\left(5 + \frac{Kr^2}{R^2}\right) + \left(1 + \frac{Kr^2}{R^2}\right)^3 \alpha}\ , \tag{4.40}$$

and

$$\frac{dp_\perp}{d\rho} = \frac{\frac{dp_\perp}{dr}}{\frac{d\rho}{dr}} \tag{4.41}$$

where $\frac{d\rho}{dr}$ and $\frac{dp_\perp}{dr}$ are given by expressions (4.29) and (4.34).

The condition $0 \leq \frac{dp_r}{d\rho}|_{(r=0)} \leq 1$ gives the following bounds on p_0 with $\alpha \geq 0$ and $K > 1$,

$$0 < p_0 \leq \frac{5(K-1)K + 2\alpha}{2K}. \tag{4.42}$$

Moreover, $0 \leq \frac{dp_r}{d\rho}|_{(r=R)} \leq 1$ leads to the following inequality

$$0 < p_0 \leq \alpha(K+1)^2 + \frac{(K-1)K(K+5)}{2(K+1)}. \tag{4.43}$$

Further, $0 \leq \frac{dp_\perp}{d\rho}|_{(r=0)} \leq 1$, give the following bounds for K, α and p_0.

$$1 < K < 3.34441, \tag{4.44}$$

$$0 \leq \alpha < \frac{1}{4}(K-1)^2, \tag{4.45}$$

and

$$2(3K+1) - \sqrt{12\alpha + 33K^2 + 30K + 1} \leq p_0 \leq 2(3K+1) - \sqrt{8\alpha + 13K^2 + 50K + 1}. \tag{4.46}$$

Moreover at the boundary ($r = R$), we have the following restrictions on K, α and p_0.

$$1 < K < 16.4118, \tag{4.47}$$

$$0 \leq \alpha < \frac{3K^3 + 20K^2 + 31K + 10}{(K+1)^2(7K+5)} - \sqrt{\frac{16K^6 + 48K^5 - 99K^4 + 948K^3 + 2054K^2 + 1044K + 85}{(K+1)^4(7K+5)^2}} \tag{4.48}$$

and

$$0 < p_0 \leq \frac{1}{8\alpha + 8\alpha K^2 - 8K^2 + 16\alpha K + 24K - 80} \times \Big(-5\alpha^2 + 20\alpha - 7\alpha^2 K^4 + 6\alpha K^4 + K^4 - 26\alpha^2 K^3 + 46\alpha K^3 - 12K^3 - 36\alpha^2 K^2 + 102\alpha K^2 - 78K^2 - 22\alpha^2 K + 82\alpha K + 92K - 3 \Big). \tag{4.49}$$

The necessary condition for the model to represent a stable relativistic star is that $\Gamma > \frac{4}{3}$ throughout the star. $\Gamma > \frac{4}{3}$ at $r = 0$ gives a bound on p_0 with $K > 1$ and $\alpha \geq 0$,

$$p_0 > \frac{2\alpha + K^2 - K}{3K}. \tag{4.50}$$

The upper limits of α in the inequalities (4.27), (4.31), (4.35), (4.39), and (4.45) for different permissible values of K are shown in Table 4.1. It can be noticed that the

smallest bound for α is given by (4.31).

The lower bounds of p_0 are calculated from (4.46) and (4.50). The upper bounds of p_0 are calculated from (4.32),(4.37),(4.42), (4.43), (4.46) & (4.49). They are listed in Table 4.2. The required lower bound for p_0 can be as taken as the largest values listed for each K and the upper bound can be taken as the least values listed for each K.

Table 4.1: The upper limits of α for different permissible values of K.

	Inequality Numbers				
K	(4.27)	(4.31)	(4.35)	(4.39)	(4.45)
1.8001	0.4898	0.0150	0.9999	7.9882	0.1600
1.9001	0.5244	0.0179	0.9405	7.8029	0.2025
2.0001	0.5556	0.0209	0.8888	7.6282	0.2501
2.1001	0.5838	0.0239	0.8439	7.4632	0.3026
2.2001	0.6094	0.0270	0.8047	7.3072	0.3601
2.3001	0.6327	0.0301	0.7704	7.1594	0.4226
2.4001	0.6540	0.0333	0.7405	7.0192	0.4901
2.5001	0.6735	0.0364	0.7143	6.8861	0.5626
2.6001	0.6914	0.0396	0.6913	6.7594	0.6401
2.7001	0.7078	0.0427	0.6713	6.6388	0.7226
2.8001	0.7230	0.0459	0.6537	6.5239	0.8101
2.9001	0.7370	0.0490	0.6384	6.4142	0.9026
3.0001	0.7500	0.0521	0.6250	6.3093	1.0001
3.1001	0.7621	0.0552	0.6133	6.2091	1.1026
3.2001	0.7733	0.0583	0.6032	6.1131	1.2101
3.3001	0.7837	0.0613	0.5944	6.0211	1.3226
3.3401	0.7876	0.0625	0.5912	5.9853	1.3690

Similarly the lower bound for p_0 can be easily seen from the next Table 4.2.

4.5 Application to Compact Stars

We shall use the charged anisotropic model on pseudo-spheroidal spacetime to strange star models whose mass and size are known. Consider the pulsar 4U 1820-30 whose estimated mass and radius are $1.58M_{\odot}$ and $9.1km$. If we use these estimates

Table 4.2: For a fixed value 0.05 of α from the above Table 4.1, the lower and upper limits of p_0 for different permissible values of K.

	Inequality Numbers							
	Lower Bounds		Upper Bounds					
K	(4.46)	(4.50)	(4.32)	(4.37)	(4.42)	(4.43)	(4.46)	(4.49)
1.8001	0.0517	0.2852	-0.4458	0.8001	2.0280	2.1409	1.2451	1.8315
1.9001	0.0685	0.3176	-0.4425	0.9001	2.2766	2.4551	1.4281	2.2249
2.0001	0.0860	0.3500	-0.4333	1.0001	2.5252	2.7837	1.6147	2.6409
2.1001	0.1042	0.3826	-0.4178	1.1001	2.7741	3.1262	1.8045	3.0756
2.2001	0.1229	0.4152	-0.3957	1.2001	3.0230	3.4824	1.9972	3.5253
2.3001	0.1421	0.4479	-0.3666	1.3001	3.2720	3.8520	2.1925	3.9860
2.4001	0.1618	0.4806	-0.3302	1.4001	3.5211	4.2349	2.3902	4.4537
2.5001	0.1819	0.5134	-0.2862	1.5001	3.7702	4.6308	2.5901	4.9247
2.6001	0.2023	0.5462	-0.2343	1.6001	4.0195	5.0395	2.7921	5.3952
2.7001	0.2231	0.5790	-0.1740	1.7001	4.2688	5.4610	2.9959	5.8619
2.8001	0.2442	0.6119	-0.1051	1.8001	4.5181	5.8951	3.2015	6.3216
2.9001	0.2655	0.6449	-0.0271	1.9001	4.7675	6.3416	3.4086	6.7715
3.0001	0.2871	0.6778	0.0601	2.0001	5.0169	6.8005	3.6173	7.2091
3.1001	0.3089	0.7108	0.1570	2.1001	5.2664	7.2716	3.8273	7.6325
3.2001	0.3309	0.7438	0.2639	2.2001	5.5159	7.7549	4.0386	8.0398
3.3001	0.3531	0.7768	0.3811	2.3001	5.7654	8.2502	4.2511	8.4296
3.3401	0.3620	0.7900	0.4310	2.3401	5.8652	8.4517	4.3365	8.5804

in (4.25) with $\alpha = 0.05$, we get $K = 2.718$ which is well inside the permitted limits of K. Similarly by taking the estimated masses and radii of some well-known pulsars like PSR J1903+327, 4U 1608-52, Vela X-1, SMC X-4 and Cen X-3, we have calculated the values of K with $\alpha = 0.05$ for each of these stars. These estimates together with some relevant physical quantities like the central density ρ_c, surface density ρ_R, the compactification factor $u = \frac{M}{R}$, $\frac{dp_r}{d\rho}_{(r=0)}$ and the charge Q inside the star are displayed in Table 4.3. From this table it is evident that charged anisotropic models can accommodate the observational data of pulsars recently given by Gangopadhyay et al. [2013].

Table 4.3: Estimated physical values based on the observational data with $\alpha = 0.05$ fixed.

STAR	**K**	**M** ($\mathbf{M_\odot}$)	**R** (**Km**)	$\rho_{\mathbf{c}}$ (**MeV fm**$^{-3}$)	$\rho_{\mathbf{R}}$ (**MeV fm**$^{-3}$)	$\mathbf{u}(=\frac{\mathbf{M}}{\mathbf{R}})$	$\left(\frac{\mathbf{dp_r}}{\mathbf{d}\rho}\right)_{\mathbf{r=0}}$	**Q** **Coulombs**
4U 1820-30	2.718	1.58	9.1	1875.15	240.29	0.256	0.251	2.36×10^{20}
PSR J1903+327	2.781	1.667	9.438	1806.35	226.58	0.261	0.242	2.45×10^{20}
4U 1608-52	3.010	1.74	9.31	2095.78	243.66	0.276	0.214	2.42×10^{20}
Vela X-1	2.969	1.77	9.56	1947.00	229.38	0.273	0.218	2.48×10^{20}
SMC X-4	2.230	1.29	8.831	1425.58	218.84	0.300	0.350	2.29×10^{20}
Cen X-3	2.502	1.49	9.178	1610.99	223.03	0.239	0.287	2.38×10^{20}

4.6 Validation of Model for 4U 1820-30

In order to examine the nature of physical quantities throughout the distribution, we have considered a particular pulsar 4U 1820-30, whose tabulated mass and radius are $M = 1.58M_\odot$, and $R = 9.1km$ respectively. From Table 4.3 it can be noticed that the corresponding values of $K = 2.718$ with $\alpha = 0.05$. We have shown the variations of density and pressures in both the charged and uncharged cases in Figure 4.1, Figure 4.2 and Figure 4.3. It can be noticed that the density is decreasing radially outward. Similarly the radial pressure p_r and transverse pressure $p_\perp$ are decreasing radially outward.

The variation of anisotropy shown in Figure 4.4 is initially decreasing with negative values reaches minimum and then increases. The square of sound speed in the radial and transverse direction (i.e. $\frac{dp_r}{d\rho}$ and $\frac{dp_\perp}{d\rho}$) are shown in Figure 4.5 and Figure 4.6 respectively and found that they are less than 1, showing that the causality condition is fulfilled throughout. The graph of $\rho - p_r - 2p_\perp$ against radius is plotted in Figure 4.7. It can be observed that it is non-negative for $0 \leq r \leq R$ and hence strong energy condition is satisfied throughout the star.

A necessary condition for the exact solution to represent stable relativistic star is that the relativistic adiabatic index given by $\Gamma = \frac{\rho+p_r}{p_r}\frac{dp_r}{d\rho}$ should be greater than $\frac{4}{3}$.

The variation of adiabatic index throughout the star is shown in Figure 4.8 and it is found that $\Gamma > \frac{4}{3}$ (Knutsen [1988a]) throughout the distribution both in charged and uncharged case. For a physically acceptable relativistic star the gravitational redshift must be positive and finite at the centre and on the boundary. Further it should be a decreasing function of r (Murad [2013a]). Figure 4.9 shows that this is indeed the case. For a physically acceptable charged distribution, the electric field intensity E should be an increasing function of r (Murad [2013a]). The variation of E^2 against r is displayed in Figure 4.10. E^2 is found to be radially increasing throughout the distribution. The model reduces to the uncharged anisotropic distribution given by Thomas and Pandya [2015a] when $\alpha = 0$.

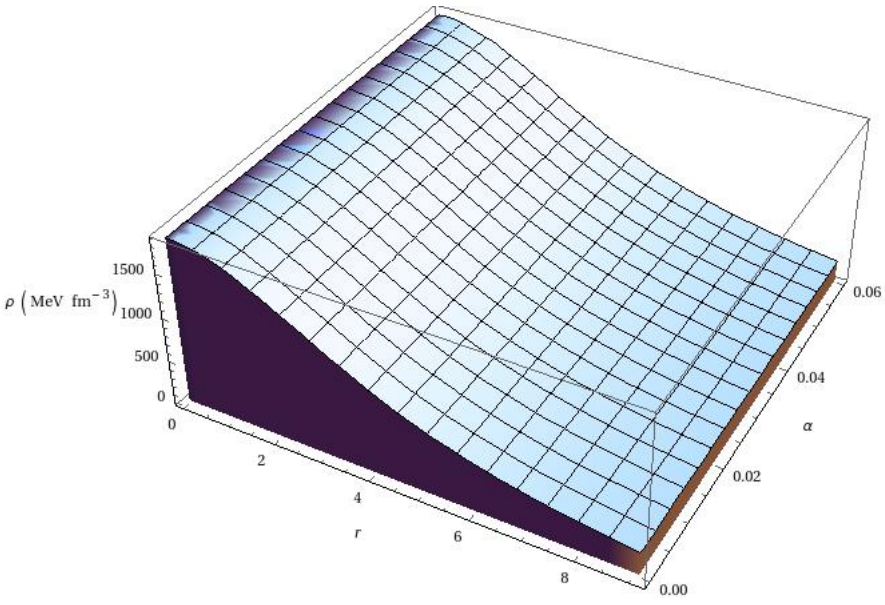

Figure 4.1: Variation of density against radial parameter r and charge parameter α for $K = 2.718$.

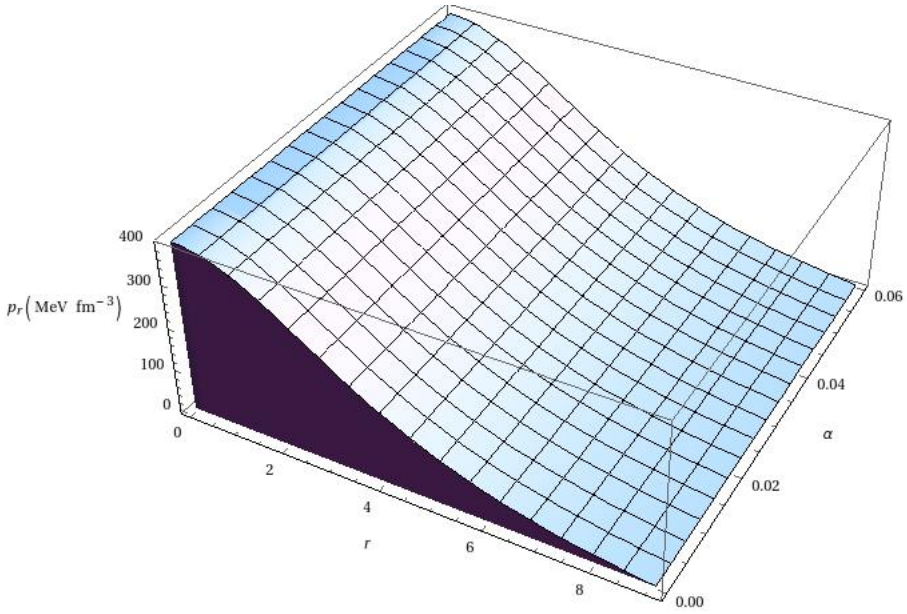

Figure 4.2: Variation of radial pressures against radial parameter r and charge parameter α for $K = 2.718$.

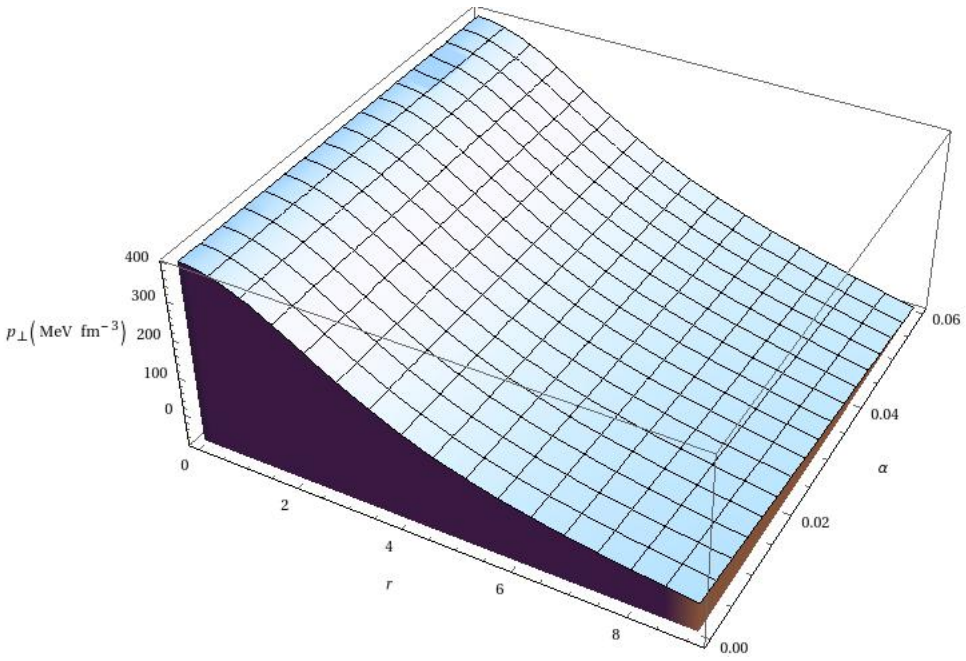

Figure 4.3: Variation of transverse pressures against radial parameter r and charge parameter α for $K = 2.718$.

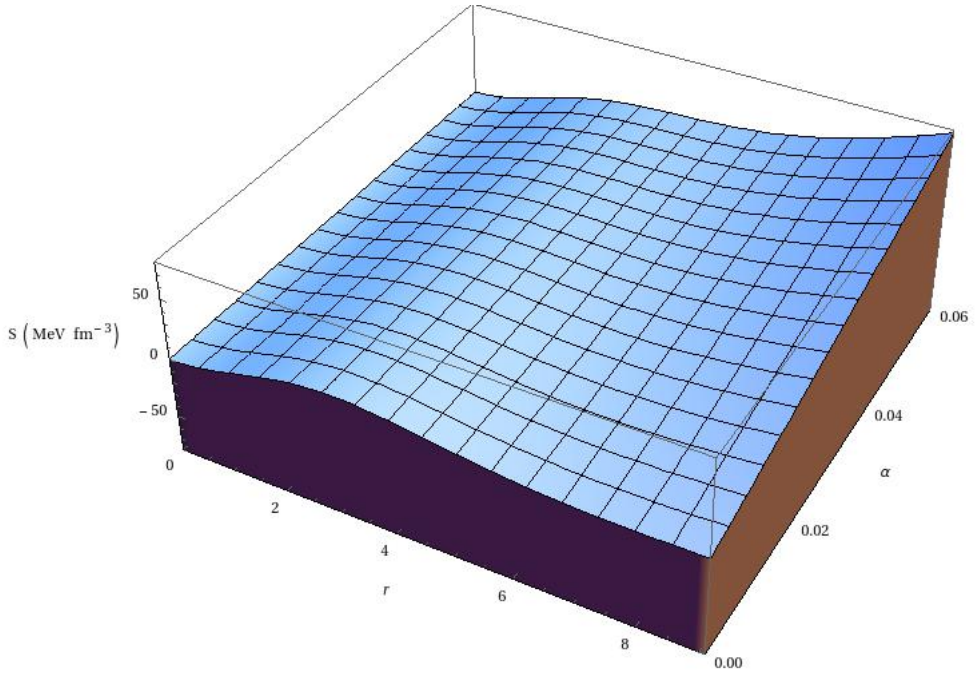

Figure 4.4: Variation of anisotropy against radial parameter r and charge parameter α for $K = 2.718$.

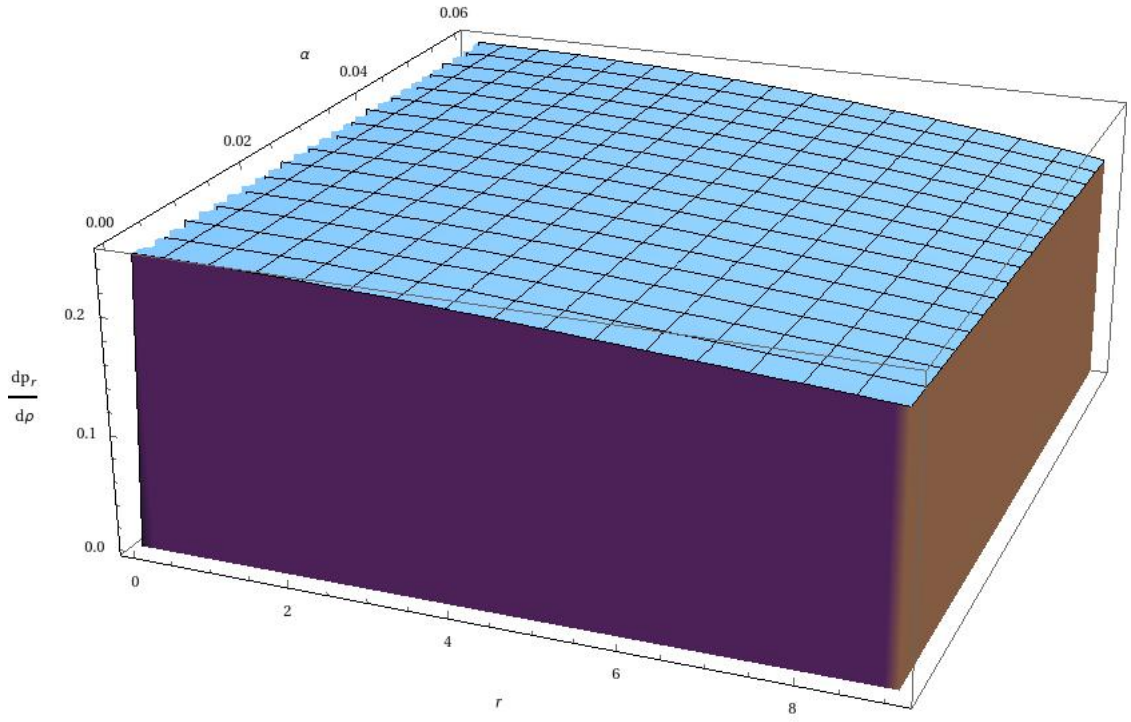

Figure 4.5: Variation of $\frac{1}{c^2}\frac{dp_r}{d\rho}$ against radial parameter r and charge parameter α for $K = 2.718$.

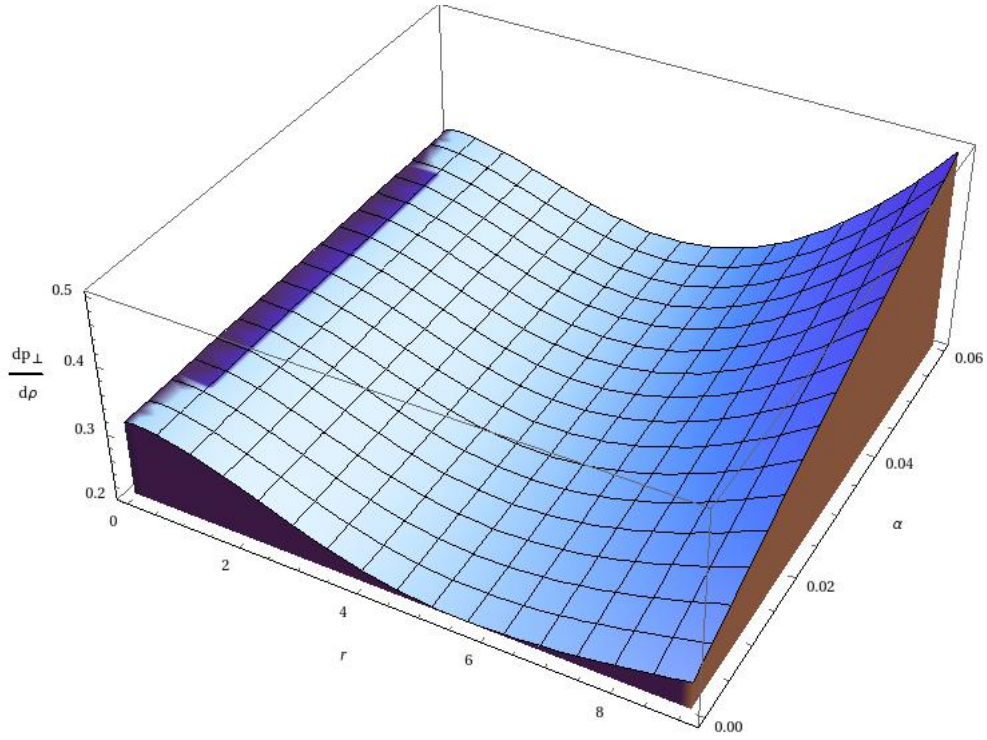

Figure 4.6: Variation of $\frac{1}{c^2}\frac{dp_\perp}{d\rho}$ against radial parameter r and charge parameter α for $K = 2.718$.

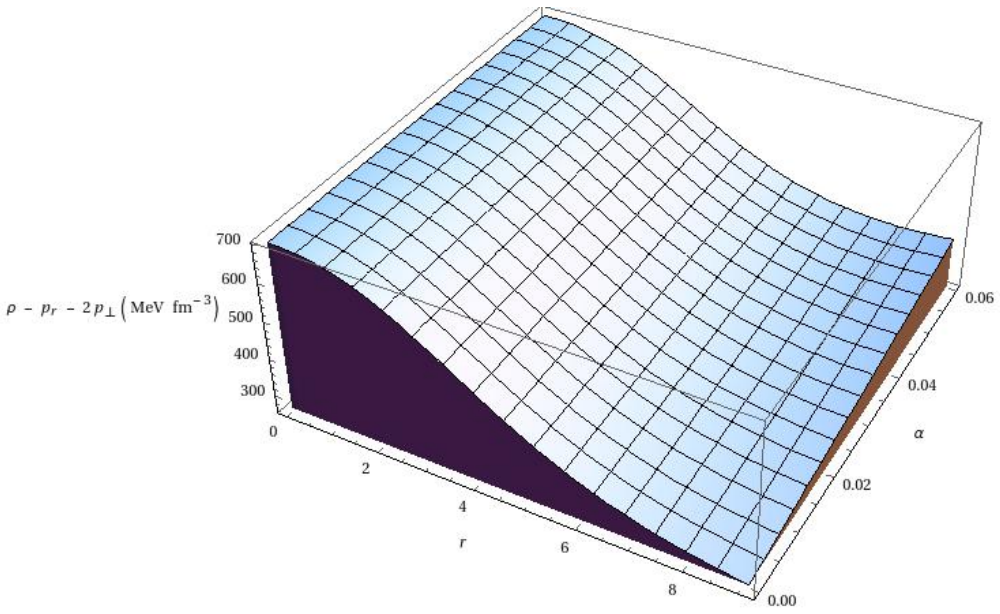

Figure 4.7: Variation of strong energy condition against radial parameter r and charge parameter α for $K = 2.718$.

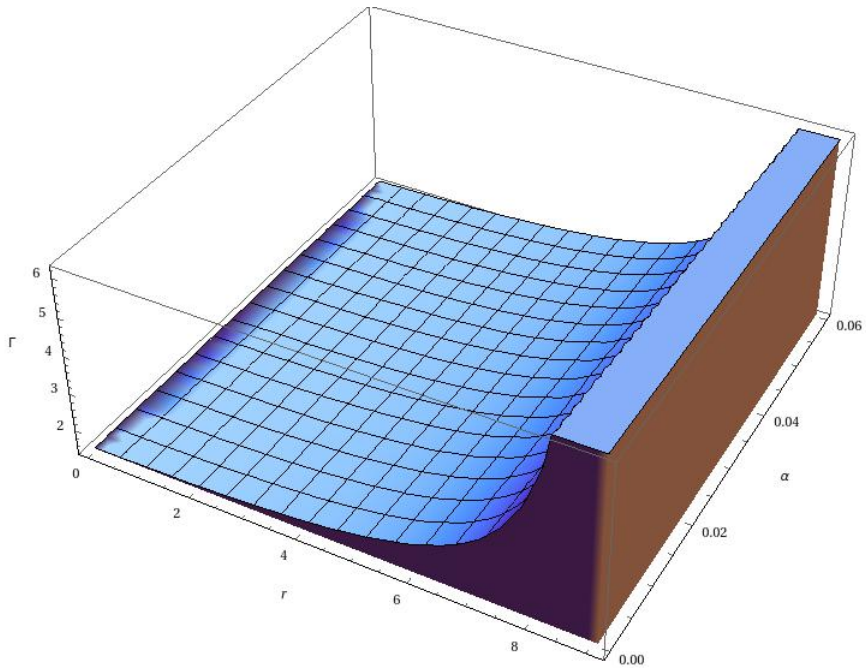

Figure 4.8: Variation of Γ against radial parameter r and charge parameter α for $K = 2.718$.

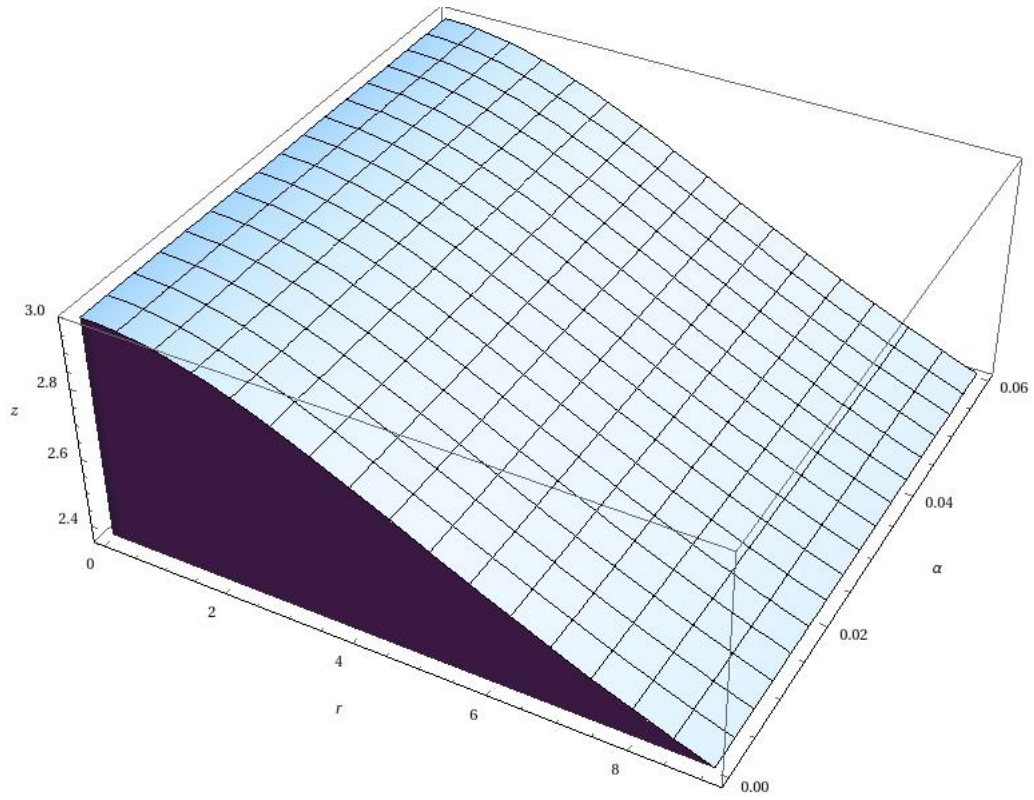

Figure 4.9: Variation of gravitational redshift against radial parameter r and charge parameter α for $K = 2.718$.

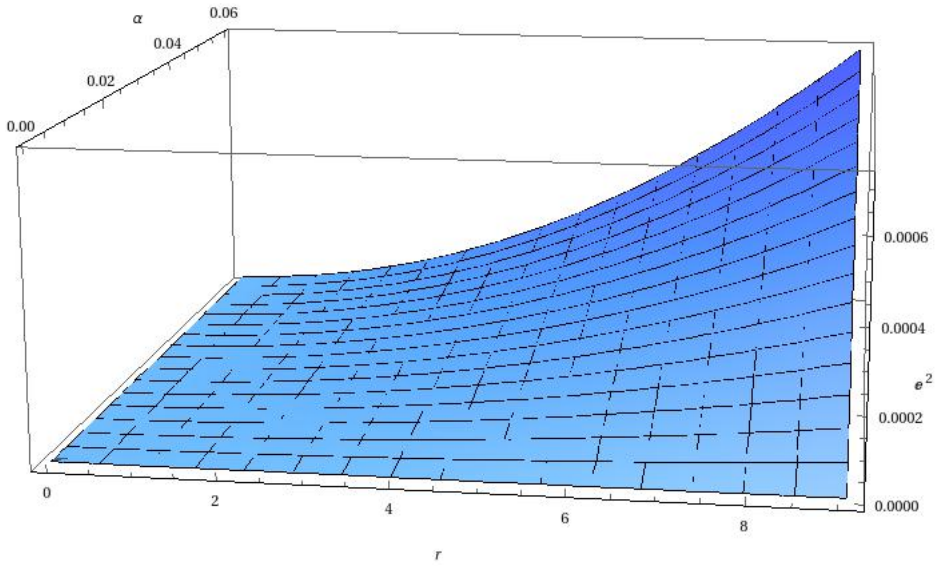

Figure 4.10: Variation of E^2 against radial parameter r and charge parameter α for $K = 2.718$.

4.7 Charged Anisotropic Model 2

We shall assume the following expressions for p_r and E.

$$8\pi p_r = \frac{K-1}{R^2}\frac{1-\frac{r^2}{R^2}}{\left(1+K\frac{r^2}{R^2}\right)^2}, \tag{4.51}$$

$$E^2 = \frac{\alpha\,(K-1)}{R^2}\frac{\frac{r^2}{R^2}}{\left(1+K\frac{r^2}{R^2}\right)}. \tag{4.52}$$

It can be noticed from equation (4.51) that p_r vanishes at $r = R$ and hence we take the geometric parameter R as the radius of distribution. Further $p_r \geq 0$ for all values of r in the range $0 \leq r \leq R$. It can also be noted that E^2 is regular at $r = 0$. On substituting the values of p_r and E^2 in (4.14) we obtain, after a lengthy calculation

$$e^{\nu} = CR^{\frac{\left[K^2-(2+\alpha)K+\alpha+1\right]}{K}}\left(1+K\frac{r^2}{R^2}\right)^{\left(\frac{K+\alpha+1}{2K}\right)}\left(1+\frac{r^2}{R^2}\right)^{\frac{K-\alpha-3}{2}}, \tag{4.53}$$

where C is a constant of integration. Hence, the spacetime metric takes the explicit form

$$\begin{aligned} ds^2 &= CR^{\frac{\left[K^2-(2+\alpha)K+\alpha+1\right]}{K}}\left(1+K\frac{r^2}{R^2}\right)^{\left(\frac{K+\alpha+1}{2K}\right)}\left(1+\frac{r^2}{R^2}\right)^{\frac{K-\alpha-3}{2}}dt^2 \\ &\quad -\left(\frac{1+K\frac{r^2}{R^2}}{1+\frac{r^2}{R^2}}\right)dr^2 - r^2\left(d\theta^2+\sin^2\theta d\phi^2\right). \end{aligned} \tag{4.54}$$

The constant of integration C can be evaluated by matching the interior spacetime metric with Riessner-Nordström metric

$$ds^2 = \left(1-\frac{2m}{r}+\frac{q^2}{r^2}\right)dt^2 - \left(1-\frac{2m}{r}+\frac{q^2}{r^2}\right)^{-1}dr^2 - r^2\left(d\theta^2+\sin^2\theta d\phi^2\right), \tag{4.55}$$

across the boundary $r = R$. This gives

$$M = \frac{R}{2}\frac{[K^2 + \alpha(K-1) - 1]}{(1+K)^2}, \tag{4.56}$$

and

$$C = R^{\frac{-\left[K^2-(2+\alpha)K+\alpha+1\right]}{K}} (1+K)^{-\left(\frac{3K+\alpha+1}{2K}\right)} 2^{\left(\frac{\alpha-K+5}{2}\right)}. \tag{4.57}$$

Here M denotes the total mass of the charged anisotropic distribution.

4.8 Physical Requirements and Bounds for Parameters

The gradient of radial pressure is obtained from equation (4.51) in the form

$$8\pi\frac{dp_r}{dr} = -\frac{2r(K-1)}{R^4}\frac{1+2K-K\frac{r^2}{R^2}}{\left(1+K\frac{r^2}{R^2}\right)^3} < 0. \tag{4.58}$$

It can be noticed from equation (4.58) that the radial pressure is a decreasing function of r. Now, equation (4.13) gives the density of the distribution as

$$8\pi\rho = \left(\frac{K-1}{R^2}\right)\frac{3+(K-\alpha)\frac{r^2}{R^2}}{\left(1+K\frac{r^2}{R^2}\right)^2}. \tag{4.59}$$

The conditon $\rho(r=0) > 0$ is clearly satisfied and $\rho(r=R) > 0$ gives the following inequality connecting α and K.

$$0 \leq \alpha < 3 + K. \tag{4.60}$$

Differentiating (4.59) with respect to r, we get

$$8\pi\frac{d\rho}{dr} = -\frac{2r(K-1)}{R^4}\frac{5K+\alpha+K(K-\alpha)\frac{r^2}{R^2}}{\left(1+K\frac{r^2}{R^2}\right)^3}. \tag{4.61}$$

It is observed that $\frac{d\rho}{dr}(r=0)=0$ and $\frac{d\rho}{dr}(r=R)<0$ leads to the inequality

$$K^2 - K(\alpha-5) + \alpha \geq 0. \tag{4.62}$$

The inequality (4.62) together with the condition $K>1$ give a bound for α as

$$0 \leq \alpha < \frac{K(K+5)}{K-1}. \tag{4.63}$$

The expression for $p_\perp$ is

$$8\pi p_\perp = \frac{4K-4+X_1\frac{r^2}{R^2}+X_2\frac{r^4}{R^4}+X_3\frac{r^6}{R^6}}{R^2\left(4+Y_1\frac{r^2}{R^2}+Y_2\frac{r^4}{R^4}+Y_3\frac{r^6}{R^6}+4K^3\frac{r^8}{R^8}\right)}, \tag{4.64}$$

where, $X_1 = 4K^2+(-12\alpha-16)K+12\alpha+12$, $X_2 = 6K^3+(-10\alpha-22)K^2+(4\alpha+14)K+6\alpha+2$, $X_3 = K^4+(-2\alpha-4)K^3+(\alpha^2+2\alpha+6)K^2+(-2\alpha^2-2\alpha-4)K+\alpha^2+2\alpha+1$, $Y_1 = 12K+4$, $Y_2 = 12K^2+12K$ and $Y_3 = 4K^3+12K^2$.

The condition $p_\perp > 0$ at the boundary $r=R$ imposes a restriction on K and α respectively given by

$$K > 2\sqrt{3}-1 \tag{4.65}$$

and

$$0 \leq \alpha < \frac{10+5K+K^2}{K-1} - \sqrt{\frac{89+102K+57K^2+8K^3}{(K-1)^2}}. \tag{4.66}$$

The expression for $\frac{dp_\perp}{dr}$ is given by

$$\frac{dp_\perp}{dr} = \frac{-r\left(8K^2+(12\alpha+8)K-12\alpha-16+A_1\frac{r^2}{R^2}+A_2\frac{r^4}{R^4}+A_3\frac{r^6}{R^6}+A_4\frac{r^8}{R^8}\right)}{R^4\left(2+B_1\frac{r^2}{R^2}+B_2\frac{r^4}{R^4}+B_3\frac{r^6}{R^6}+B_4\frac{r^8}{R^8}+B_5\frac{r^{10}}{R^{10}}+2K^4\frac{r^{12}}{R^{12}}\right)}, \tag{4.67}$$

where, $A_1 = -4K^3+(28-4\alpha)K^2+(16\alpha-20)K-12\alpha-4$, $A_2 = 3K^4+(-4\alpha-4)K^3+(-3\alpha^2-28\alpha-30)K^2+(6\alpha^2+44\alpha+36)K-3\alpha^2-12\alpha-5$, $A_3 = 10K^4+(-16\alpha-36)K^3+(-2\alpha^2+4\alpha+16)K^2+(4\alpha^2+16\alpha+12)K-2\alpha^2-4\alpha-2$, $A_4 = K^5+(-2\alpha-4)K^4+(\alpha^2+2\alpha+6)K^3+(-2\alpha^2-2\alpha-4)k^2+\alpha^2+2\alpha+1$, $B_1 = 8k+4$, $B_2 = 12K^2+16K+2$, $B_3 = 8K^3+24K^2+8K$, $2K^4+16K^3+12K^2$ and $B_4 = 4K^4+8K^3$.

The value of $\frac{dp_\perp}{dr} = 0$ at the origin and $\frac{dp_\perp}{dr}(r=R) < 0$ gives the following bounds for K and α respectively

$$2\sqrt{13}-5 < K < 5 \tag{4.68}$$

and

$$0 \leq \alpha < \frac{K^3+10K^2+25K-20}{K^2-6K+5}+\sqrt{\frac{16K^5+233K^4+252K^3+278K^2-788K+265}{(K^2-6K+5)^2}} \tag{4.69}$$

In order to examine the strong energy condition, we evaluate the expression $\rho-p_r-2p_\perp$ at the centre and on the boundary of the star. It is found that

$$(\rho-p_r-2p_\perp)(r=0) = 0, \tag{4.70}$$

and $(\rho-p_r-2p_\perp)(r=R) > 0$ gives the bound on K and α, namely

$$1 < K < 1+2\sqrt{6} \tag{4.71}$$

$$0 \leq \alpha < \frac{8+3K+K^2}{K-1} + \sqrt{\frac{41+46K+49K^2+8K^3}{(K-1)^2}}. \tag{4.72}$$

The expressions for adiabatic sound speed $\frac{dp_r}{d\rho}$ and $\frac{dp_\perp}{d\rho}$ in the radial and transverse directions, respectively, are given by

$$\frac{dp_r}{d\rho} = \frac{1+2K-K\frac{r^2}{R^2}}{5k+\alpha+K(K-\alpha)\frac{r^2}{R^2}}, \tag{4.73}$$

and

$$\begin{aligned}\frac{dp_\perp}{d\rho} &= \frac{\left(1+K\frac{r^2}{R^2}\right)^3\left[8K^2+(12\alpha+8)K-12\alpha-16+C_1\frac{r^2}{R^2}+C_2\frac{r^4}{R^4}+C_3\frac{r^6}{R^6}+C_4\frac{r^8}{R^8}\right]}{2(K-1)\left[5K+\alpha+K(K-\alpha)\frac{r^2}{R^2}\right]} \\ &\times\frac{1}{\left[2+D_1\frac{r^2}{R^2}+D_2\frac{r^4}{R^4}+D_3\frac{r^6}{R^6}+D_4\frac{r^8}{R^8}+D_5\frac{r^{10}}{R^{10}}+2K^4\frac{r^{12}}{R^{12}}\right]},\end{aligned} \tag{4.74}$$

where, $C_1 = -4K^3+(18-4\alpha)K^2+(16\alpha-20)K-12\alpha-4$, $C_2 = 3K^4+(-4\alpha-4)K^3+(-3\alpha^2-28\alpha-30)K^2+(6\alpha^2+44\alpha+36)K-3\alpha^2-12\alpha-5$, $C_3 = 10K^4+(-16\alpha-36)K^3+(-2\alpha^2+4\alpha+16)K^2+(4\alpha^2+16\alpha+12)K-2\alpha^2-4\alpha-2$, $C_4 = K^5+(-2\alpha-4)K^4+(\alpha^2+2\alpha+6)K^3+(-2\alpha^2-2\alpha-4)K^2+(\alpha^2+2\alpha+1)K$, $D_1 = 8K+4$, $D_2 = 12K^2+16K+2$, $D_3 = 8K^3+24K^2+8K$, $D_4 = 2K^4+16K^3+12K^2$ and $D_5 = 4K^4+8K^3$.

The condition $0 \leq \frac{dp_r}{d\rho} \leq 1$ is evidently satisfied at the centre whereas at the boundary it gives a restriction on α as

$$0 \leq \alpha < \frac{K^2+4K-1}{K-1},\ K>1. \tag{4.75}$$

Further $\frac{dp_\perp}{d\rho} \leq 1$ at the centre will lead to the following inequalities

$$K > \frac{4}{3} \tag{4.76}$$

and

$$0 \leq \alpha < \frac{1}{2}(3K-4). \tag{4.77}$$

Moreover at the boundary ($r = R$), we have the following restrictions on K and α.

$$-5+2\sqrt{13} \leq K < 5 \tag{4.78}$$

and

$$0 \leq \alpha \leq \frac{K^3+10K^2+25K-20}{K^2-6K+5} + \sqrt{\frac{16K^5+233K^4+252K^3+278K^2-788K+265}{\left(K^2-6K+5\right)^2}}, \tag{4.79}$$

The necessary condition for the model to represent a stable relativistic star is that $\Gamma > \frac{4}{3}$ throughout the star. $\Gamma > \frac{4}{3}$ at $r = 0$ gives a bound on α which is identical to (4.60). Further, $\Gamma \to \infty$ as $r \to R$ and hence the condition is automatically satisfied. It can be noticed that $E = 0$ at $r = 0$, showing the regularity of the charged distribution.

The upper limits of α in the inequalities (4.60), (4.63), (4.66), (4.69), (4.72), (4.75) and (4.77) for different permissible values of K are shown in Table 4.4. It can be noticed that for $2.4641 < K \leq 3.7641$ the bound for α is $0 \leq \alpha \leq 0.6045$.

4.9 Application to Compact Stars and Discussion

In order to compare the charged anisotropic model on pseudo-spheroidal spacetime with observational data, we have considered the pulsar PSR J1614-2230 whose estimated mass and radius are $1.97M_{\odot}$ and 9.69 km. On substituting these values in equation (4.56) we have obtained the values of adjustable parameters K and α as $K = 3.58524$ and $\alpha = 0.292156$ respectively which are well inside their permitted

Table 4.4: The upper limits of α for different permissible values of K.

	Inequality Numbers						
K	(4.60)	(4.63)	(4.66)	(4.75)	(4.77)	(4.69)	(4.72)
2.4641	5.4641	12.5622	**0.0000**	10.1962	1.6962	0.0802	30.9893
2.5041	5.5041	12.4932	**0.0170**	10.1635	1.7562	0.0938	30.6186
2.6041	5.6041	12.3445	**0.0599**	10.0977	1.9062	0.1287	29.7861
2.7041	5.7041	12.2250	**0.1036**	10.0514	2.0562	0.1648	29.0693
2.8041	5.8041	12.1299	**0.1480**	10.0213	2.2062	0.2021	28.4488
2.9041	5.9041	12.0552	**0.1931**	10.0048	2.3562	0.2405	27.9094
3.0041	6.0041	11.9980	**0.2388**	10.0000	2.5062	0.2798	27.4388
3.1041	6.1041	11.9557	**0.2852**	10.0052	2.6562	0.3201	27.0271
3.2041	6.2041	11.9263	**0.3321**	10.0189	2.8062	0.3612	26.6662
3.3041	6.3041	11.9082	**0.3795**	10.0401	2.9562	0.4030	26.3495
3.4041	6.4041	11.8998	**0.4275**	10.0679	3.1062	0.4457	26.0714
3.5041	6.5041	11.9002	**0.4760**	10.1015	3.2562	0.4890	25.8272
3.6041	6.6041	11.9082	**0.5251**	10.1401	3.4062	0.5330	25.6130
3.7041	6.7041	11.9230	**0.5745**	10.1833	3.5562	0.5776	25.4254
3.7541	6.7541	11.9327	**0.5995**	10.2065	3.6312	0.6001	25.3407
3.7641	6.7641	11.9348	**0.6045**	10.2112	3.6462	0.6047	25.3244

limits. Similarly assuming the estimated masses and radii of some well known pulsars like 4U 1820-30, PSR J1903+327, 4U 1608-52, Vela X-1, PSR J1614-2230, Cen X-3, we have displayed the values of the parameters K and α, the central density ρ_c, surface density ρ_R, the compactification factor $u = \frac{M}{R}$, $\frac{dp_r}{d\rho}(r = 0)$ and charge Q inside the star in Table 4.5. From the table it is clear that our model is in good agreement with the most recent observational data of pulsars given by Gangopadhyay et al. [2013].

Table 4.5: Estimated physical values based on the observational data

STAR	**K**	**M** ($\mathbf{M_\odot}$)	**R** (**Km**)	$\rho_\mathbf{c}$ (**MeV fm^{-3}**)	$\rho_\mathbf{R}$ (**MeV fm^{-3}**)	$\mathbf{u}(=\frac{\mathbf{M}}{\mathbf{R}})$	$\left(\frac{\mathbf{dp_r}}{\mathbf{d\rho}}\right)_{\mathbf{r=0}}$	**Q Coulomb**
4U 1820-30	2.815	1.58	9.1	1980.14	250.46	0.256	0.461	4.031×10^{20}
PSR J1903+327	2.880	1.667	9.438	1906.90	235.92	0.261	0.460	4.184×10^{20}
4U 1608-52	3.122	1.74	9.31	2212.22	252.97	0.276	0.455	4.127×10^{20}
Vela X-1	3.078	1.77	9.56	2054.99	238.25	0.273	0.456	4.240×10^{20}
PSR J1614-2230	**3.585**	**1.97**	**9.69**	**2487.35**	**248.17**	**0.300**	**0.448**	$\mathbf{4.262 \times 10^{20}}$
Cen X-3	2.589	1.49	9.178	1705.08	233.65	0.239	0.466	4.044×10^{20}

In order to examine the nature of physical quantities throughout the distribution, we have considered a particular star PSR J1614-2230, whose tabulated mass and radius are $M = 1.97M_{\odot},\ R = 9.69\ km$. Choosing $K = 3.58524$ and $\alpha = 0.292156$, we have shown the variations of density and pressures in both the charged and uncharged cases in Figure 4.11, Figure 4.12 and Figure 4.13. It can be noticed that the pressure is decreasing radially outward. The density in the uncharged case is always greater than the density in the charged case. Similarly the radial pressure p_r and transverse pressure $p_\perp$ are decreasing radially outward. Similar to that of density, p_r and $p_\perp$ in the uncharged case accommodate more values compared to charged case.

The variation of anisotropy shown in Figure 4.14 is initially decreasing with negative values reaches a minimum and then increases. In this case also anisotropy takes lesser values in the charged case compared to uncharged case. The square of sound in the radial and transverse direction (i.e. $\frac{dp_r}{d\rho}$ and $\frac{dp_\perp}{d\rho}$) are shown in Figure 4.15 and Figure 4.16 respectively and found that they are less than 1. The graph of $\rho - p_r - 2p_\perp$ against radius is plotted Figure 4.17. It can be observed that it is non-negative for $0 \leq r \leq R$ and hence strong energy condition is satisfied throughout the star.

A necessary condition for the exact solution to represent stable relativistic star is that the relativistic adiabatic index given by $\Gamma = \frac{\rho+p_r}{p_r}\frac{dp_r}{d\rho}$ should be greater than $\frac{4}{3}$. The variation of adiabatic index throughout the star is shown in Figure 4.18 and it is found that $\Gamma > \frac{4}{3}$ throughout the distribution both in charged and uncharged case. Though we have not assumed any equation of state in the explicit form $p_r = p_r(\rho)$ and $p_\perp = p_\perp(\rho)$, we have shown the relation between $p_r, p_\perp$ against ρ in the graphical form as displayed in Figure 4.19 and Figure 4.20. For a physically acceptable relativistic star the gravitational redshift must be positive and finite at the centre and on the boundary. Further it should be a decreasing function of r.

Figure 4.21 shows that this is indeed the case. Finally we have plotted the graph of E^2 against r which is displayed in Figure 4.22. Initially E^2 increases from 0 and reaches a maximum values and then decreases radially outward. The model reduces to the uncharged anisotropic distribution given by Ratanpal et al. [2016] when $\alpha = 0$.

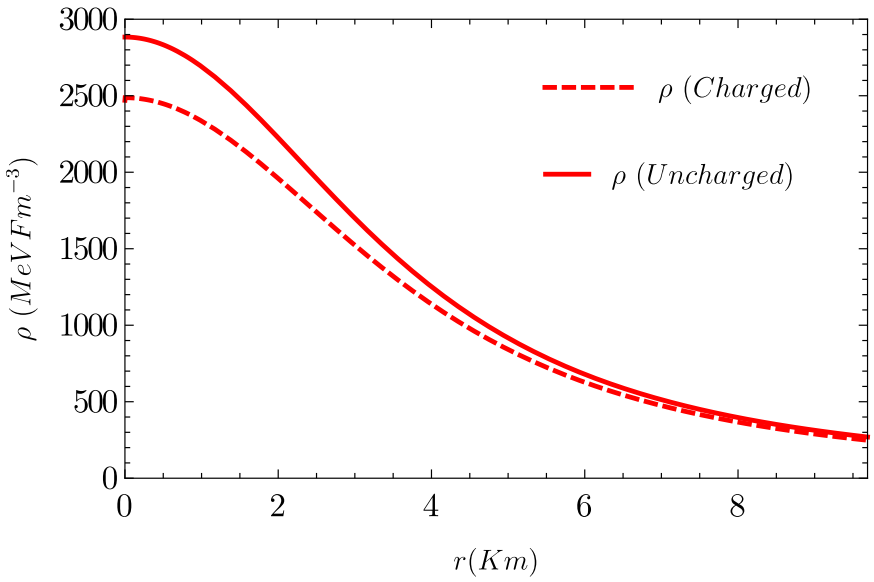

Figure 4.11: Variation of density against radial variable r.

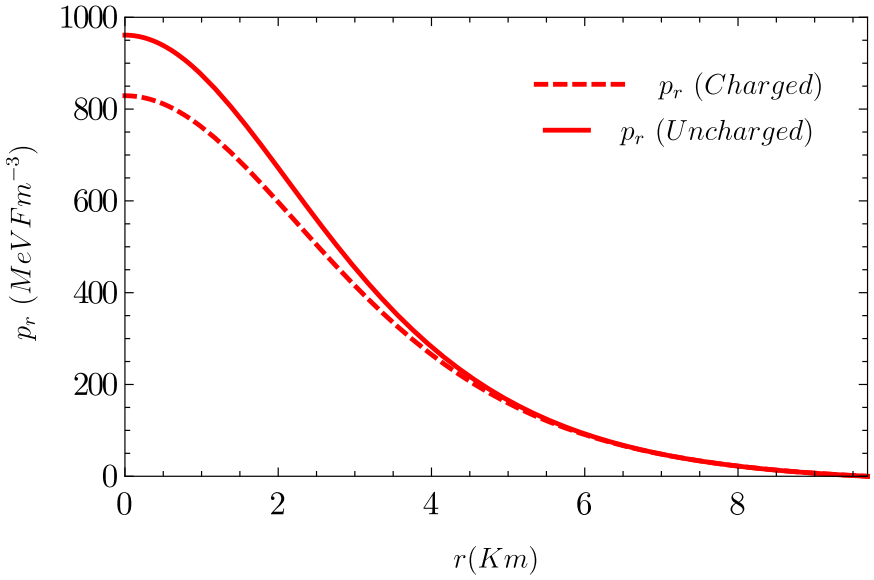

Figure 4.12: Variation of radial pressures against radial variable r.

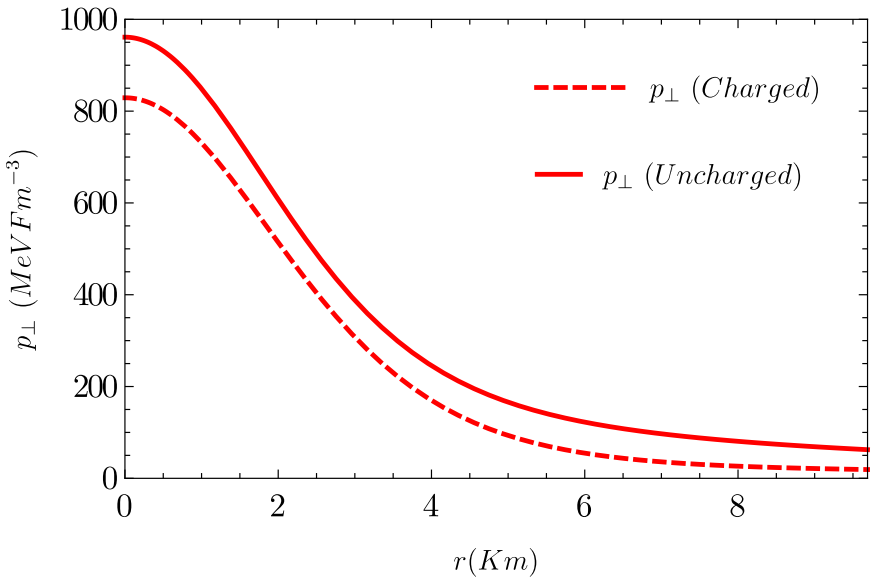

Figure 4.13: Variation of transverse pressures against radial variable r

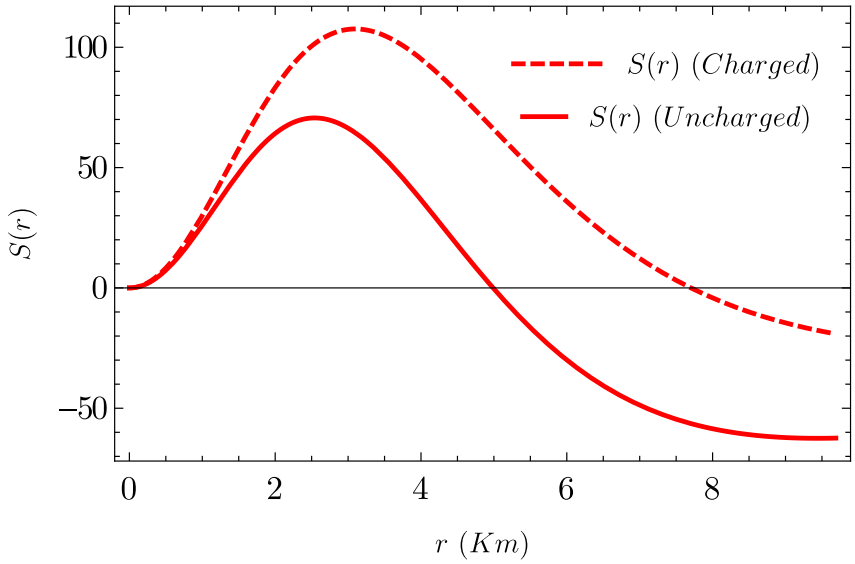

Figure 4.14: Variation of anisotropies against radial variable r.

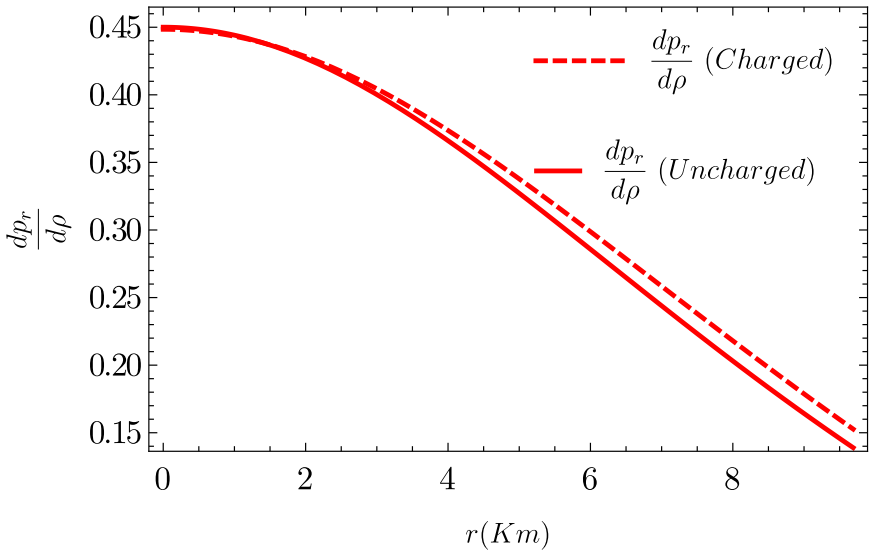

Figure 4.15: Variation of $\frac{1}{c^2}\frac{dp_r}{d\rho}$ against radial variable r.

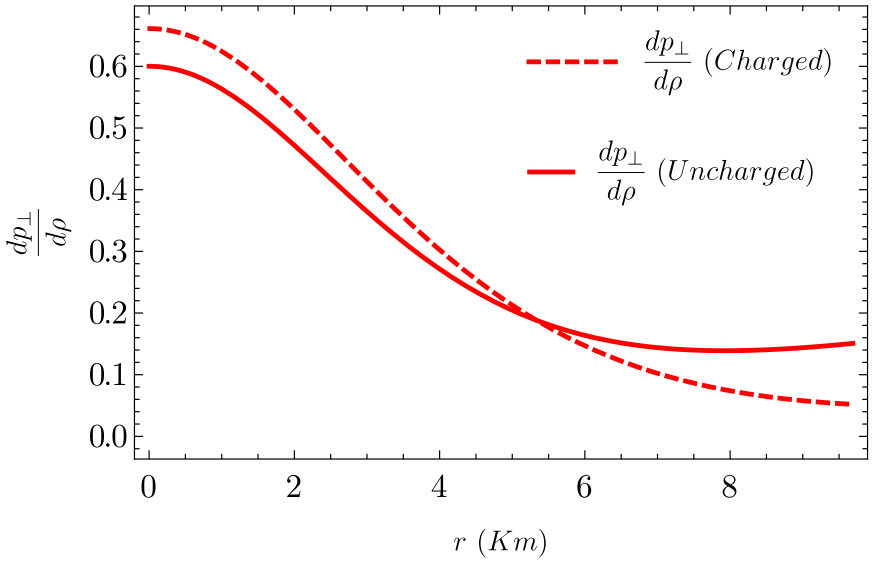

Figure 4.16: Variation of $\frac{1}{c^2}\frac{dp_\perp}{d\rho}$ against radial variable r.

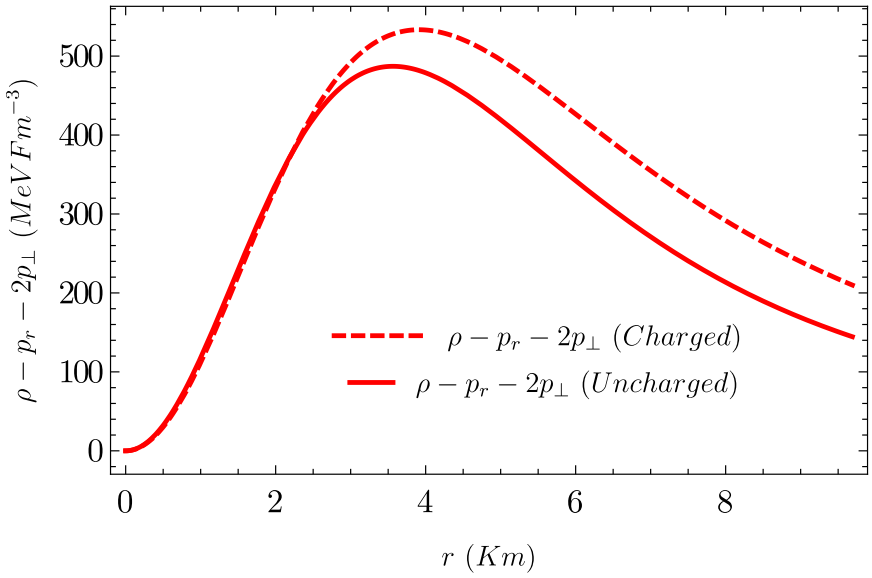

Figure 4.17: Variation of strong energy condition against radial variable r.

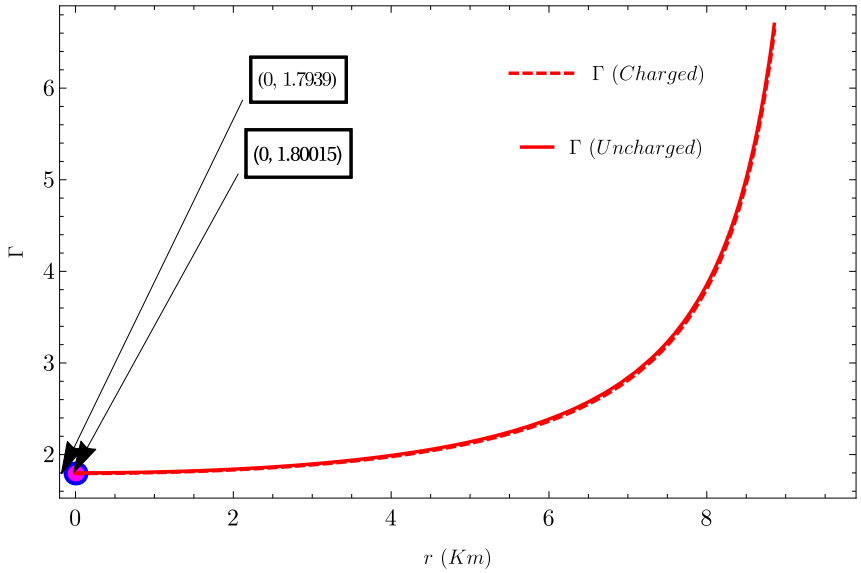

Figure 4.18: Variation of Γ against radial variable r.

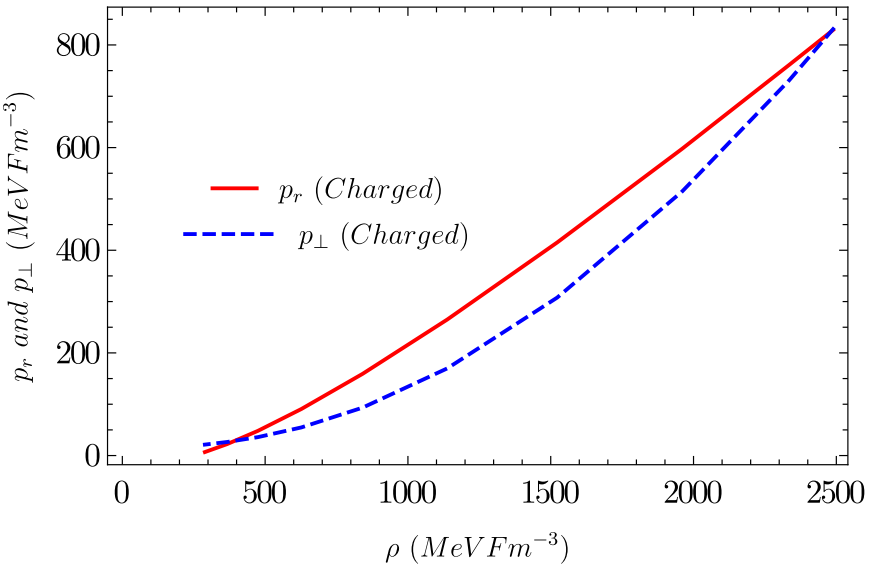

Figure 4.19: Variation of pressures against density for charged case.

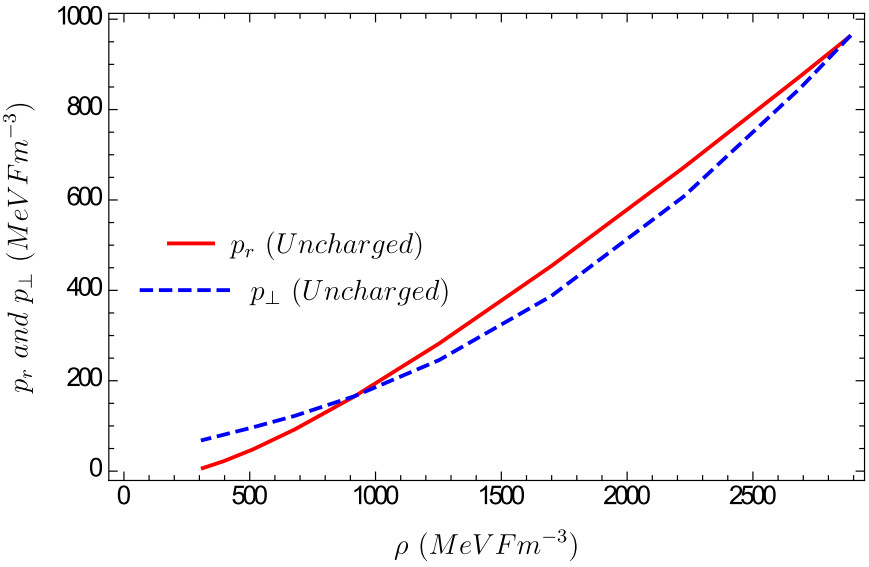

Figure 4.20: Variation of pressures against density for uncharged case.

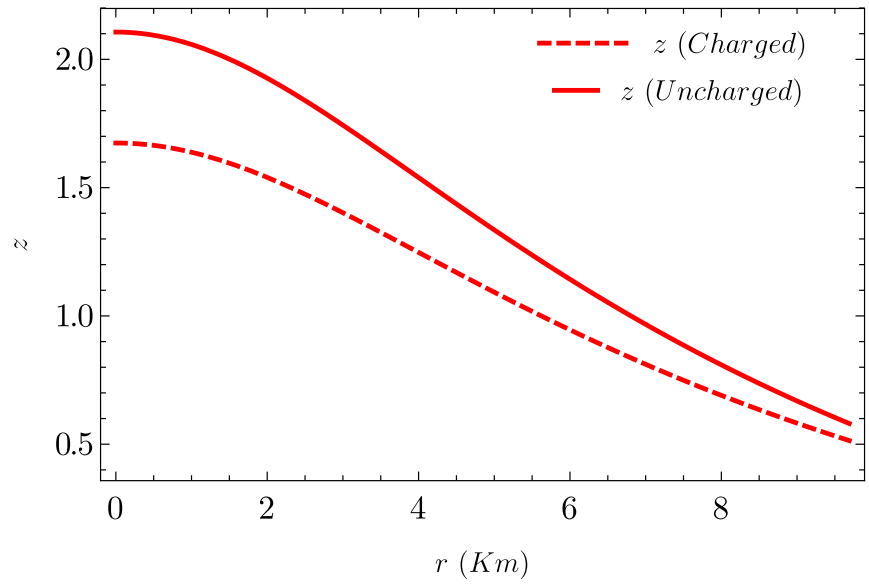

Figure 4.21: Variation of gravitational redshift against radial variable r.

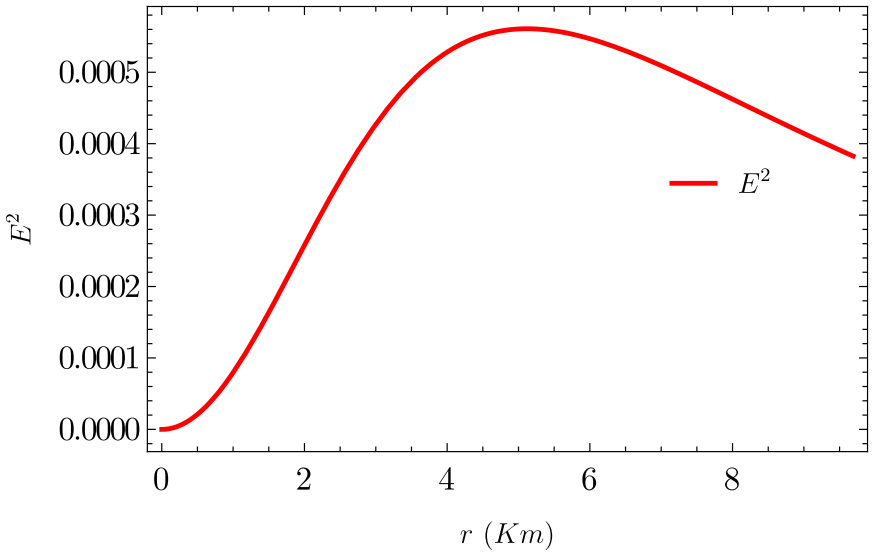

Figure 4.22: Variation of E^2 against radial variable r.